International Arab Conference on Information Technology (ACIT'2016)

Positive definite kernels for identification and equalization of Indoor Broadband Radio Access Network

Mohammed Boutalline[1], Mohamed Gouskir[2], Jilali Antari[3], Belaid Bouikhalene[1], Said Safi[1]
[1]Laboratory for Interdisciplinary Research in Science and Techniques, Polydisciplinary Faculty, Sultan Moulay Slimane University, Beni Mellal, Morocco
[2]Laboratory of Sustainable Development, Faculty of Science and Techniques, Sultan Moulay Slimane University, Beni Mellal, Morocco
[3]Polydisciplinary Faculty of Taroudant, Ibn Zohr University, 32/S Agadir 80000, Morocco
boutalline@gmail.com

Abstract :*We consider a transmission system, where the transmitted symbols are subject of inquiry. The kernels-based algorithms are of great importance to many problems. The channel identification and equalization operate by a proposed algorithm based on positive kernel method for multi-carrier code division multiple (MC-CDMA) system. Two practical selective frequency fading channels are considered; they are called broadband radio access network (BRAN A and BRAN B) normalized by ETSI. To conceive the proposed algorithm, we focused on the positive definite kernels. Numerical simulations show that the algorithm confirms the good performance for different Signal to Noise Ratio (SNR). We use zero forcing (ZF) and minimum mean square error (MMSE) equalizers for the equalization MC-CDMA system.*

Keywords :*Positive Kernel method, Identification, Equalization, MC-CDMA systems, BRAN Channel.*

1. Introduction

Several studies using different techniques have identified the finite impulse response (FIR) channel [6]. Some classes of algorithms for channel estimation are based on the iterative strategy while other ones focus on the structural methods of the received observation [5, 33, 19, 1]. Many developed algorithms have led to significant results in the identification problem in Single-Input Single-Output (SISO). [26] and [24] exploited the techniques based on Higher Order Statistics (HOS) for channel identification and equalization in a scenario where the input of the channel was not available for processing at the receiver. [15] concentrated on supervised equalization of a Single-Input Single-Output (SISO) linear communication channel using generalized orthogonal basis (GOB).

Recently, the machine learning community has shown great interest in kernel methods where the first use is the exploitation of the Support Vector Machine(SVM) in [32]. Moreover, several studies considered kernel-base algorithms [20, 4, 31, 21, 30].

To evaluate the efficiency of the algorithm, we propose measured frequency selective fading channel, the so-called Broadband Radio Access Network (BRAN). These channel models have been standardized by ETSI in the BRAN project ([7] and [8]), whose aim was to define the physical layer and control systems HIPERLAN/2 wireless local area network broadband. This standard is based on the use of a $20MHz$ band allocated to a carrier frequency of $f\_c = 5.2\ GHz$. Each model consists of $N\_t = 18$ targets whose amplitude delays τ_i following an exponential decay for each target i. This standardization is five scenarios of propagation. These define the interior propagation phenomena building up environments in open areas.

The goal of this paper is to propose an algorithm based on kernel positive method. This algorithm allows estimating the impulse response of the channel model BRAN A and B. In the equalization section, we performed the received data for signal-carrier MC-CDMA systems by ZF and MMSE equalizers.

2. Problem Statement

We propose the transmission of i.i.d zero-mean symbols with unit energy, across a linear, discrete, time-invariant finite impulse response (FIR) channel drive by input symbols (Fig.1).

The following Eq.(1) describes the output $x(n)$ which it represents the convolution product:

$$\begin{aligned} x(n) &= h_p * s(n) \\ &= \sum_{i=0}^{P} h(n)s(n-i) \end{aligned} \quad (1)$$

where $h_p = [h(1), h(2), \ldots, h(P)]$ represents the impulse response coefficients of Non-minimum phase (NMP) channel and P order of FIR system.

In noisy environment case, the output system is affected by an additive white Gaussian noise with $E\{w^2(n)\} = \sigma^2$. The observed output at the receiver $\{r(n)\}$ is given by:

$$r(n) = x(n) + w(n) \quad (2)$$

The input sequence, $\{s(n)\}$, is independent and identically distributed (i.i.d) zero mean and non-Gaussian. The system is causal, i.e $h(n) = 0$ for $i \le 0$ and $i \ge P$, where channel identification problem is to estimate h_p only from the received observation $r(n)$.

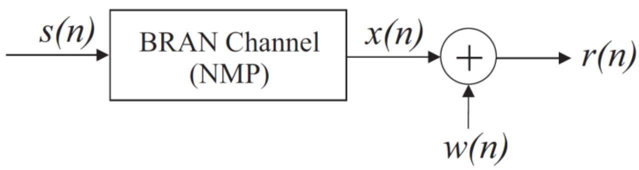

Figure 1: Channel model.

3. Kernel Methods

Kernel methods have recently been developed in the Machine Learning Community. They are powerful techniques based on nonlinear transformation of the data x living in a space X into a high dimensional reproducing kernel Hilbert space H (RKHS) through a non-linear map ϕ where the transformed data $\phi(x)$ is linearly separable. In this feature space, inner products can be calculated by using a positive definite kernel function satisfying Mercer's condition [32]: $k(x, x') = \langle x, x' \rangle$.

The main idea, known as the "kernel trick", allows working in feature space by replacing all inner products with kernels in the input space. Gaussian kernel is the most widely used Mercer kernel.

$$k(x, x') = \exp\left(\frac{|x - x'|}{2\sigma^2}\right), \quad (3)$$

where σ is the kernel width.

Providing a number of samples of N input-output data pairs $\{x(n), d(n)\}$ where $n = 1, \ldots, N$, The cost function to be minimized is based on kernel ridge regression [27] Eq. (4):

$$J = \sum_{n=1}^{N} |r(n) - \Phi(s(n))|^{\bullet} + cw^{\bullet} w \quad (4)$$

where c is a Tikhonov regularization constant. Note that w is not calculated in the high-dimensional feature space. Fortunately, the Representer Theorem allos w to be obtained as a kernel expansions in terms of transformed data $\Phi(x(n))$ We used a portion of the data as a training sequence to calculate w using the kernel trick and also reduce computational complexity.

$$w = \sum_{m=1}^{M} \alpha_m \Phi\left(x_m^t\right) \quad (5)$$

The matrix notation is obtained from Eq. (4) and Eq. (5).

$$J = \|r - K\alpha\|^2 + c\alpha^{\bullet} K_t \alpha, \quad (6)$$

Where K is the kernel matrix and $\alpha = \left(K^{\bullet} K + cK_t\right)^{-1} K^{\bullet} r$.

4. Proposed Algorithm

Consider the output $r(n)$ of the system in Fig. 1:

$$r(n) = h(n) * f\left(x(n)\right) + w(n) \quad (7)$$

Where $h = \left[h(1), h(2), \ldots, h(p)\right]$ represents the channel impulse response with memory P and the operator $*$ refers to the convolution.

In order to identify the channel parameters, we propose to minimize the cost function:

$$J = \|r - h * K\alpha\|^2 + c_\alpha \alpha^{\bullet} K_t \alpha + c_h h^{\bullet} h \quad (8)$$

Where c_α and c_h are constants. However, it is possible to obtain the coefficients $\hat{\alpha}$ if the estimated parameters $\hat{h}$ were available. The term $c_h h^{\bullet} h$ can be eliminated because it does not affect the minimization of Eq. 8. By doing so, the cost function can be written as:

$$J_\alpha = \|r - h * K\alpha\|^2 + c_\alpha \hat{\alpha}^{\bullet} K_t \hat{\alpha} \quad (9)$$

The proposed algorithm that can identify the channel parameters is as follows:

Step 1: Generate the kernel matrix K and initialize $\hat{h}$ by the Eq. (10)

$$\hat{h} = (X^{\bullet} X + c_h I)^{-1} X^{\bullet} r \quad (10)$$

where X contains vectors of the data $x(n)$.

Step 2: As the cost function J isn't converged, we update each iteration K_h and $\hat{\alpha}$ by Eq. (11) and (Eq.12) respectively:

$$K_h = \hat{h} * K \quad (11)$$

we introduce α by :

$$\hat{\alpha} = (K_h^{\bullet} K_h + c_\alpha K_s)^{-1} K_h^{\bullet} r \quad (12)$$

Step 3: Still within the current iteration, we obtain the value of $K_\alpha = K\hat{\alpha}$ and the estimated parameters $\hat{h}$ as follows:

$$K_\alpha = \begin{bmatrix} k_\alpha(1) & 0 & \cdots & 0 \\ k_\alpha(2) & k_\alpha(1) & \cdots & 0 \\ \vdots & \vdots & \ddots & \vdots \\ k_\alpha(N) & k_\alpha(N-1) & \cdots & k_\alpha(N-P+1) \end{bmatrix} \quad (13)$$

Where K_α is an $N \times P$ matrix.

And also the impulse responses of the channel is :

$$\hat{h} = \left(K_\alpha^{\bullet} K_\alpha + c_h I\right)^{-1} K_\alpha^{\bullet} r \quad (14)$$

In an iterative manner, we can ensure the convergence of the proposed algorithm because it minimizes the cost function every time and because it alternates to find the approximation of h by update the coefficients α .

5. MC-CDMA System

The radio communication station in Fig. 2 shows the general organization of a synchronous downlink between a transmitter and N_U mobile terminals based on the MC-CDMA technique [14, 10, 13, 16]. The series-parallel conversion in the transmitter shows that each subcarrier is modulated by each user data multiplied by each of the chips of their spreading sequence. To remedy the disruptions introduced by the transmission channel, it is necessary to apply an equalization system. There are two types of sensors, single-user detectors and multi-user detectors [18]. In the first case, only the sequence of the user concerned is assumed to be known; the interference due to other users is then considered as jammers. In the other, the sequences of all users are known, the multiple access interferences are then considered deterministic signals.Thus, in case N_U users are active, the received signal can be written as:

$$r(t) = (h*s)(t) + w(t) \quad (15)$$

$$r(t) = \frac{1}{\sqrt{N_C}} \sum_{l=0}^{L-1} \sum_{j=0}^{N_U-1} \sum_{p=0}^{N_C-1} \beta_l(t) e^{j(2\pi v_l t + \theta_l(t))}. \quad (16)$$

$$x_j c_{p,j} e^{2j\pi(p-N_C/2)\frac{t-\tau_l}{T_S}} + w(t)$$

$\theta_l(t) = -2\pi v_l \tau_l(t)$ is the displacement phase introduced by the propagation path l. To facilitate the presentation of different detection techniques, we assume a proper dimensioning of the system under study. Thus, the duration of the guard interval T_g (or T_{pc} cyclic prefix) will be sufficient, ensuring no interference between symbols and subcarriers. In addition, the duration of MC-CDMA symbol will be sufficient to consider the channel as invariant over the duration of the symbol and absence of frequency selectivity of each subcarrier. Then, the independence of random processes affecting each subcarrier is guaranteed by the time and frequency interleaving.

The time-frequency equivalence allows the modeling of the channel in the frequency domain by a set of N_c, h_p coefficient, equal to $\rho_p e^{i\varphi p}$$, assigning each subcarrier p , independent and constant over the duration of a symbol $T_s + T_g$.

Finaly, to facilitate the introduction of different detection techniques, we take L_C equal to N_C . Thus, after filtering, the baseband transposition, sampling and removing the guard interval, the expression of an MC-CDMA received symbol can be written as [29]:

$$\mathrm{r = HCx + w} \quad (17)$$

where r denotes a vector consisting of the received values for each subcarrier:

$$r = \left[r_0, \ldots, r_{N_c-1}\right]^{\bullet} \quad (18)$$

The matrix H is the matrix of the size of the channel coefficients $N_c \times N_c$. The assumptions previously made on the correct size of the system allow considering this as a diagonal matrix:

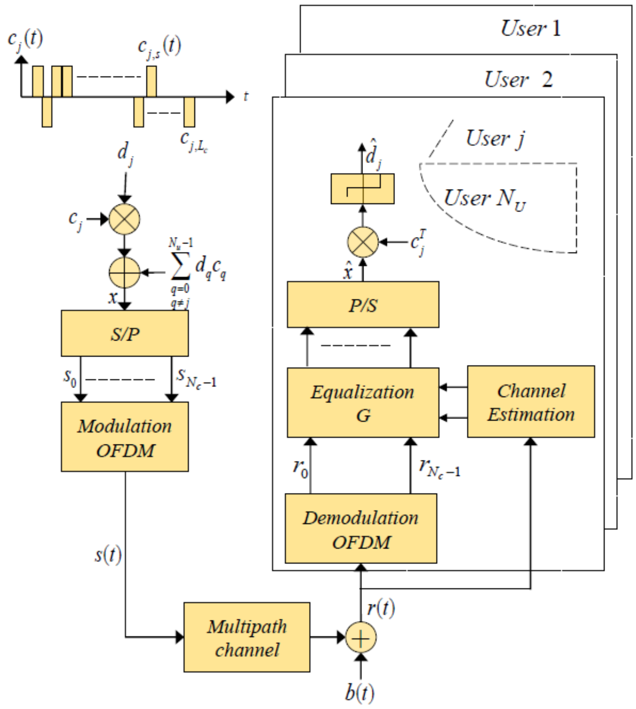

Figure 2 : Representation of a chain of radiocommunication using the MC-CDMA.

$$H = \begin{bmatrix} h_0 & 0 & \ldots & 0 \\ 0 & h_1 & \ldots & 0 \\ \vdots & \vdots & \ddots & \vdots \\ 0 & 0 & \ldots & h_{N_c-1} \end{bmatrix} \quad (19)$$

C represents the matrix of the spreadig codes. The spreading operation can be represented as the multiplication of the matrix C by the vector d which is the data of each user. Therefore, we have:

$$C=\begin{bmatrix} C_0 & \cdots & C_{N_U-1} \end{bmatrix} = \begin{bmatrix} C_{0,0} & C_{0,1} & \cdots & C_{0,N_U-1} \\ C_{1,0} & C_{1,1} & \cdots & C_{1,N_U-1} \\ \vdots & \vdots & \ddots & \vdots \\ C_{L_c-1,0} & C_{L_c-1,0} & \cdots & C_{L_c-1,N_U-1} \end{bmatrix} \quad (20)$$

with

$C_j=\left[C_{0,j},C_{1,j},\cdots,C_{(L_C-1),j}\right]^{\bullet}$ and $d=\left[d_0,\cdots,d_{N_U-1}\right]^{\bullet}$

and $w=\left[w_0,\cdots,w_{N_U-1}\right]^{\bullet}$

The vector w represents the N_c components of the noise affecting each subcarrier and can be modeled as Gaussian process additives.

In reception, we have the detectors under study based on the use of an equalization stage, the monitoring of despreader operations of the user sequence considered, and finally the binary demodulation. The performance achieved with multi-user detectors is better than that of single-user detectors, we consider first the single-user detectors to understand the principle of multi-user detectors better.

5.1. Techniques of single-user equalization for the system MC-CDMA

Single-user detectors consider only the active user signal; other users are considered as scramblers [28, 11, 22, 25]. Single-user detectors are conventionally encountered and use a linear equalization structure consisting of an equalizer into an outlet. Using the matrix notation above, it is possible to express G , the diagonal matrix made of the equalization coefficients g_p :

$$G=\begin{bmatrix} g_0 & 0 & \cdots & 0 \\ 0 & g_1 & \cdots & 0 \\ \vdots & \vdots & \ddots & \vdots \\ 0 & 0 & \cdots & g_{N_c-1} \end{bmatrix} \quad (21)$$

After equalization and spreading according to the user sequence considered C_j, the estimate of the transmitted symbol can be expressed as:

$$\begin{aligned} \hat{d}_j &= c_j^{\bullet}\hat{x} = c_j^{\bullet}Gr \\ &= c_j^{\bullet}G(HCx+w) \end{aligned} \quad (22)$$

Therefore

$$\begin{aligned} \hat{d}_j &= \sum_{p=0}^{N_C-1} C_{p,j}^2 g_p h_p x_j \\ &+ \sum_{\substack{q=0 \\ q\neq j}}^{N_U-1} \sum_{p=0}^{N_C-1} C_{p,j} C_{p,q} g_p h_p x_q \\ &+ \sum_{p=0}^{N_C-1} C_{p,j} g_p w_p \end{aligned} \quad (23)$$

In this formula (eq. 23), there are three parts. The first part forms the useful signal or data received from the current user. The second part represents multiple access interference (MAI) and is generated by the jammers. The last part of the expression is the additive white Gaussian noise weighted spreading code of the user in question and the equalization coefficient applied to each subcarrier. There are various techniques of single-user detection that can be implemented such as Maximum Ratio Combining, Equal Gain Combining, Orthogonality Restoring Combining and Minimum Mean Square Error [9]. Here, we describe the main ones.

5.2. Orthogonality Restoring Combining or Zero Forcing Algorithm

This is called zero-forcing algorithm. As in the equalization the algorithm seeks to avoid interference from other transmitters without worrying about the consequences of noise; that is, at the cost of the degradation of the SNR [23].

The equalization coefficient applied to each subcarrier is given by Eq. (24) as shown in Fig. 3:

$$g_p=\frac{1}{h_p} \quad (24)$$

with $h_p \neq 0$.

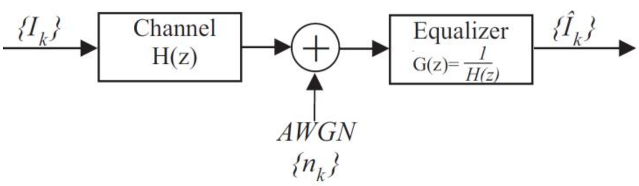

Figure 3 : Block diagram channel with zero-forcing equalizer

In this case, the expression of d_j estimate becomes:

$$\begin{aligned} \hat{d}_j &= \sum_{p=0}^{N_C-1} C_{p,j}^2 x_j + \sum_{\substack{q=0 \\ q\neq j}}^{N_U-1} \sum_{p=0}^{N_C-1} C_{p,j} C_{p,q} x_q \\ &+ \sum_{p=0}^{N_C-1} C_{p,j} \frac{1}{h_p} w_p \end{aligned} \quad (25)$$

The use of orthogonal spreading codes to the levels of the transmitter guarantees that:

$$\sum_{s=0}^{L_C-1} C_{s,j} C_{s,p} = 0, \forall j \neq q \tag{26}$$

From Eq. (25), the second term of the expression corresponding to the term of MAI is canceled. The expression then becomes:

$$\hat{x}_j = \sum_{p=0}^{N_C-1} C_{p,j}^2 x_j + \sum_{p=0}^{N_C-1} C_{p,j} \frac{1}{h_p} w_p \tag{27}$$

The performance of this technique that restores the orthogonality of spreading codes will therefore be independent of the number of users. Its defect is the amplification of the white noise term during deep fades when h_p tends to 0. In this case, the amplified noise on some carriers will degrade the overall system performance. To make up for this, it is possible to apply this technique to a certain threshold α.

For amplitudes below this threshold, a fixed value is used g_p:

$$g_p = \begin{cases} \dfrac{1}{h_p} & if \ |h_p| > \alpha \\ \xi & if \ |h_p| \leq \alpha \end{cases} \tag{28}$$

5.3. Minimum Mean Square Error

The MMSE technique achieves a compromise between minimizing multiple access interference and maximizing the signal to noise ratio [3, 17, 2]. Thus, as the name suggests, the technique aims to minimize the mean square error value for each subcarrier between the transmitted signal and the equalized signal. This leads to the expression of the coefficients g_p:

$$g_p = \frac{h_p^*}{|h_p|^2 + \dfrac{1}{\varsigma_p}} \quad , \quad with \ \varsigma_p \neq 0 \tag{29}$$

Considering that the signal is independent of the noise, and assuming that the channel power is normalized $(\varepsilon[|h_p|^2] = 1)$, the SNR per subcarrier becomes equal to:

$$\varsigma_p = \frac{\varepsilon[|x_p|^2]}{\varepsilon[|w_p|^2]}_{\varepsilon[|h_p|^2]=1} \tag{30}$$

The estimated received symbol, of symbol $\hat{d}_j$ of user j is obtained by Eq. (31) :

$$\hat{d}_j = \underbrace{\sum_{p=0}^{N_C-1} C_{p,j}^2 \frac{|h_p|^2}{|h_p|^2 + \dfrac{1}{\varsigma_p}} d_j}_{I(j=p)} + \underbrace{\sum_{\substack{q=0 \\ q\neq j}}^{N_U-1} \sum_{p=0}^{N_C-1} C_{p,j} C_{p,q} \frac{|h_p|^2}{|h_p|^2 + \dfrac{1}{\varsigma_p}} d_q}_{II(j\neq p)} + \underbrace{\sum_{p=0}^{N_C-1} C_{p,j} \frac{h_p^*}{|h_p|^2 + \dfrac{1}{\varsigma_p}} w_p}_{III} \tag{31}$$

We assume that the spreading codes are orthogonal to the levels of the transmitter, i.e.,

$$\sum_{p=0}^{N_C-1} C_{p,j} C_{q,p}, \forall j \neq q \tag{32}$$

The Eq. (31) decreases as follows:

$$\hat{d}_j = \underbrace{\sum_{p=0}^{N_C-1} C_{p,j}^2 \frac{|h_p|^2}{|h_p|^2 + \dfrac{1}{\varsigma_p}} d_j}_{I(j=p)} + \underbrace{\sum_{p=0}^{N_C-1} C_{p,j} \frac{h_p^*}{|h_p|^2 + \dfrac{1}{\varsigma_p}} w_p}_{III} \tag{33}$$

6. Simulation results

In this section, we present some simulation results to show the performance of the proposed algorithm. The normalized mean square error is used to measure the accuracy of the estimated values as noted in Eq. (34).

$$NMSE(h, \hat{h}) = \frac{1}{P} \sum_{i=1}^{P} \left(\frac{h(i) - \hat{h}(i)}{h(i)} \right)^2 \tag{34}$$

The BRAN radio channels are considered to illustrate the performance of the impulse response estimation and the strength of equalizers at the equalization part in the second experiment.

6.1. BRAN radio channels identification

We are particularly interested in two models BRAN A (inside, closed area) and BRAN B (indoor, open area). The following Eq. (35) describes the impulse response $h(n)$ of BRAN radio channel.

$$h(n) = \sum_{i=0}^{N_T} h_i \delta(n - \tau_i) \tag{35}$$

In Tables 1 and 2, we presente the values corresponding to BRAN A and BRAN B radio channels impulse response [12].

Table 1 : Delay and magnitudes of 18 targets of BRAN A radio channel

Delay τ_i [ns]	Mag.[dB]	Delay τ_i [ns]	Mag.[dB]
0	0	90	-7.8
10	-0.9	110	-4.7
20	-1.7	140	-7.3
30	-2.6	170	-9.9
40	-3.5	200	-12.5
50	-4.3	240	-13.7
60	-5.2	290	-18
70	-6.1	340	-22.4
80	-6.9	390	-26.7

Table 2 : Delay and magnitudes of 18 targets of BRAN B radio channel

Delay τ_i [ns]	Mag.[dB]	Delay τ_i [ns]	Mag.[dB]
0	-2.6	230	-5.6
10	-3.0	280	-7.7
20	-3.5	330	-9.9
30	-3.9	380	-12.1
50	0	430	-14.3
80	-1.3	490	-15.4
110	-2.6	560	-18.4
140	-3.9	640	-20.7
180	-3.4	730	-24.6

6.1.1. Channel Impulse Response Estimation of BRAN A

Fig. 4 presents the estimated magnitude and phase response of BRAN A channel using the proposed algorithm, when $SNR = 16\,dB$ and the data length $N = 1024$. The simulation results show that the magnitude impulse response of BRAN A channel is closer to the real ones when the sample size $N = 2048$ and $SNR = 16\,dB$.

Fig. 4 displays the BRAN A impulse response for $N = 2048$ as estimated by the proposed algorithm. Concerning the estimation of BRAN A channel impulse response for input symbols size $N = 2048$ and $SNR = 16\,dB$, we obtain a small difference between the estimated and the measured ones. Therefore, the proposed algorithm is closer to the performance in noisy environments.

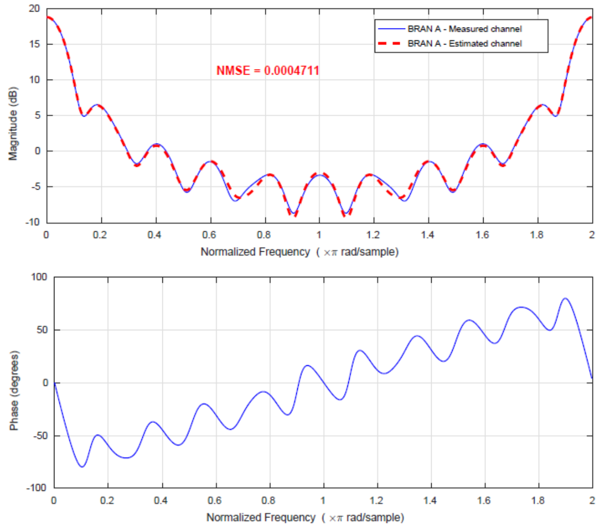

Figure 4 : Estimation of the BRAN A radio channel impulse response for a $SNR = 16\,dB$ and a data length $N = 2048$

6.1.2. Channel Impulse Response Estimation of BRAN B

Seeing that BRAN B radio channel is also composed of $N_T = 18$ parameters (Table 2) and to examine the performance of the proposed algorithm by fixing the length of the source data at $N = 2048$ and $SNR = 16\,dB$ as shown in Fig. 5.

Once again, we notice that the algorithm is similar to BRAN B channel impulse response, which is approximately close to the true one.

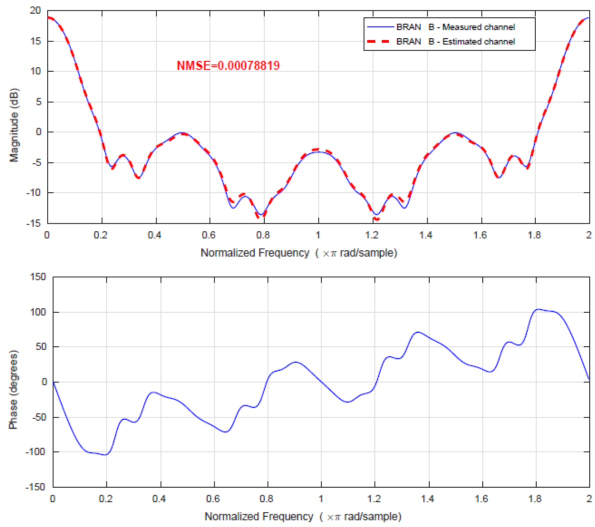

Figure 5 : Estimation of the BRAN B radio channel impulse response for a $SNR = 16\,dB$ and a data length $N = 2048$

In Fig. 6, we consider the unfavorable conditions, i.e small data ($N = 256$) the signal to noise ratio ($SNR = 0\,dB$), of the impulse response estimation using the proposed algorithm. When the output channel is more affected by the noise, i.e $SNR = 0\,dB$, we estimate the magnitude impulse response.

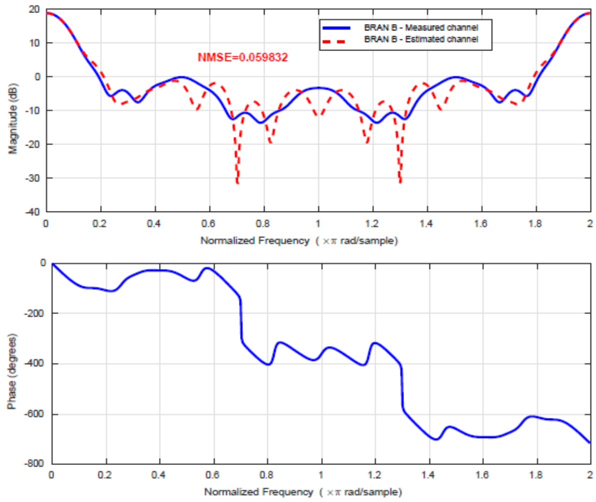

Figure 6 : Estimation of the BRAN B radio channel impulse response for a $SNR = 0\,dB$ and a data length $N = 256$

In troublesome conditions ($N = 256$ and $SNR = 0\,dB$), the obtained results are displayed in Fig. 6. We see that even if the two curves are not identical, they follow the same pace. We conclude that the proposed algorithm typically gives low state NMSEs (NMSE=0.059).

We conducted experiments on three different data sets. For every experiment, we vary the signal of noise ratio ($SNR = 0,\ 16,\ 32\,dB$) and measure the NMSE. The result is summarized in Table 3.

Table 3 : NMSE of BRAN channel Estimation for Different Samples N and Different SNR

BRAN	N	SNR [dB]	NMSE
BRAN A	512	0	$5.6197\ 10^{-3}$
		16	$6.3476\ 10^{-5}$
		32	$3.0922\ 10^{-6}$
	1024	0	$1.1112\ 10^{-3}$
		16	$6.7013\ 10^{-5}$
		32	$5.6249\ 10^{-7}$
	2048	0	$1.5682\ 10^{-3}$
		16	$1.8775\ 10^{-5}$
		32	$3.3156\ 10^{-7}$
	$2^{16} \approx \infty$	0	$2.2752\ 10^{-5}$
		16	$2.6777\ 10^{-6}$
		32	$4.1335\ 10^{-8}$
BRAN B	512	0	$6.6539\ 10^{-4}$
		16	$2.7093\ 10^{-5}$
		32	$2.1940\ 10^{-6}$
	1024	0	$6.7983\ 10^{-3}$
		16	$1.4589\ 10^{-5}$
		32	$1.0790\ 10^{-6}$
	2048	0	$2.1371\ 10^{-4}$
		16	$1.8266\ 10^{-5}$
		32	$3.5038\ 10^{-7}$
	$2^{16} \approx \infty$	0	$1.9838\ 10^{-5}$
		16	$6.0474\ 10^{-7}$
		32	$1.4662\ 10^{-8}$

Table 3 presents the NMSE between the measured channel and the estimated BRAN A channel and BRAN B channel by proposed algorithm. Averages are taken over 100 independent Monte-Carlo simulations. The results indicate that the NMSE values obtained are low in serious noise cases such as $SNR = 0\,dB$.

6.2. Equalization Performance for MC-CDMA System

In this part we evaluate the performance of the MC-CDMA systems, using the proposed algorithm for different conditions and different input signals characteristics. Random digital sequence in binary form $[0,1]$ is generated and BPSK modulation is performed on digital data. Consider a channel affected by AWGN noise so the bit error rate (BER), defined as the frequency of errors in average bit over the number of Monte Carlo runs, has been used as performance MC-CDMA.

6.2.1. MMSE and ZF Equalizers : The Case of BRAN A Channel

The zero forcing (ZF) equalization technique is applied for varying SNR from $4\,dB$ to $40\,dB$ and BER is calculated (See Fig. 7. Then, comparison is made with theoretical BER. Next, count number of bit errors for different SNR values. Afterwards, we performed MMSE equalization technique for different tap-lengths and calculated BER (See Fig. 8). Last, the comparison of BER of MMSE, ZF and theoretical value is done.

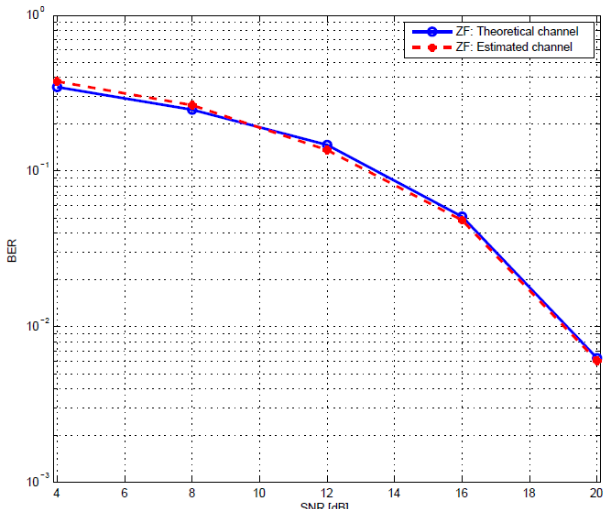

Figure 7 : Bit Error Rate for MC-CDMA (Downlink) BRAN A using ZF equalizer

The obtained BER values using ZF and MMSE equalizers are Fig. 7 and 8 respectively. We include the results for BER simulation for varying SNR which demonstrate that the estimated values are closer to the measured ones. In the case of BRAN A radio channel, we noted that the MMSE equalizer is better than the ZF method.

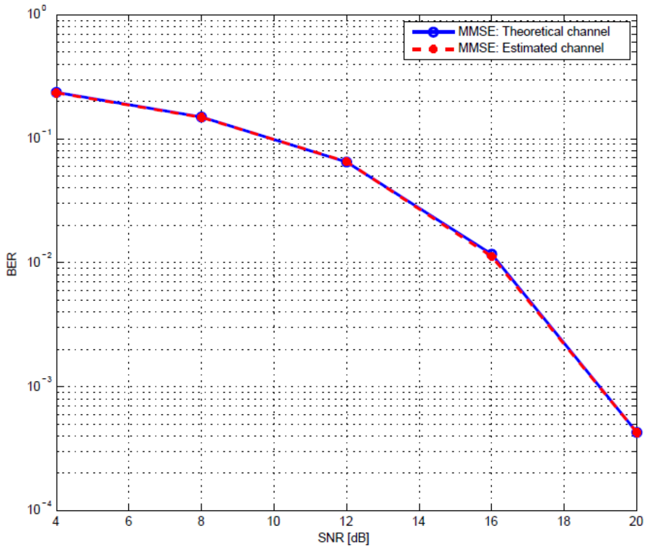

Figure 8 : Bit Error Rate for MC-CDMA (Downlink) BRAN A using MMSE equalizer

6.2.2. MMSE and ZF Equalizers : The case of BRAN B Channel

We calculated the BER of different SNR using the real and estimated BRAN A channel and we compared the performance of ZF equalizer to the performance of MMSE equalizer shown in Fig. 9 and 10 respectively.

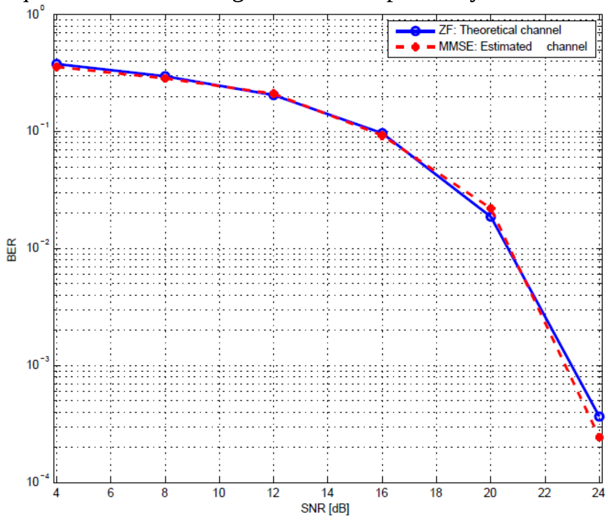

Figure 9 : Bit Error Rate for MC-CDMA (Downlink) BRAN B using ZF equalizer

In Fig. 9 and 10, we notice that the equalization gives approximately the same results obtained using the measured BRAN B values. Therefore, if $SNR = 24dB$, BER is less than 10^{-3}, but using the MMSE technique, it is less than 10^{-4}.

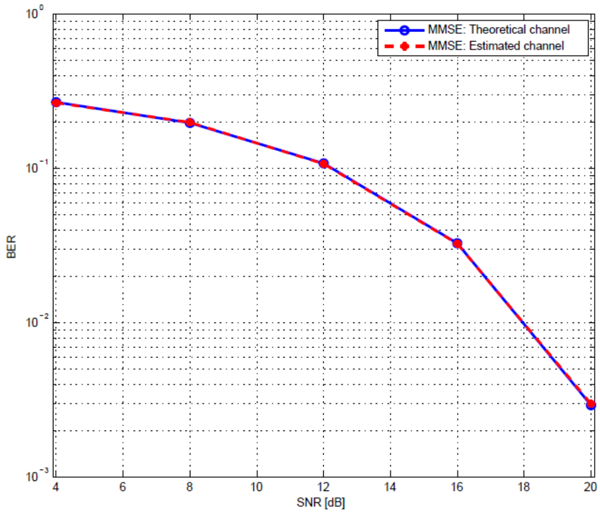

Figure 10 : Bit Error Rate for MC-CDMA (Downlink) BRAN B using MMSE equalizer

7. Conclusion

In this paper, we introduced an algorithm based on kernel positive methods. It is used to estimate channel parameters for MC-CDMA systems. The numerical results present the accuracy of the proposed algorithm for the magnitude and the phase estimation of the impulse response channel (Proakis channels, BRAN A and BRAN B) in noisy environments and as well as in small length of samples. In the part of the equalization of downlink (MC-CDMA) Systems, we have obtained good results of BER values.

Future research should focus on the performance of algorithms considered in others scenarios such as the numbers of user memory, calculating time.

References

[1] Badi, I., Boutalline, M., and Safi, S. (2013). Blind identification of transmission channel with the method of higher-order cummulants. International Journal of Advances in Science and Technology, 6(3).

[2] Baudais, J.-Y. (2001). Multicarrier spread spectrum modulation: Analysis and optimization. Theses, INSA de Rennes.

[3] Bellanger, M. (2008). High spectral resolution for future broadband wireless systems. URSI General Assembly08.

[4] Camps-Valls, G., Rojo-A lvarez, J., and Martinez-Ramon, M. (2007). Kernel methods in bioengineering, signal and image processing. Idea Group Pub.

[5] Darsena, D., Gelli, G., Paura, L., and Verde, F. (2004). Subspace-based blind channel identification of siso-fir systems with improper random inputs. Signal Processing, 84(11):2021–2039. Special Section Signal Processing in Communications.

[6] Delmas, J., Meurisse, Y., and Comon, P. (2009). Performance limits of alphabet diversities for fir siso

channel identification. Signal Processing, IEEE Transactions on, 57(1):73–82.
[7] ETSI (1999). Broadband radio acces network (bran) ; high performance radio local area network (hyperlan] type 2; requirements and archtiectures for wireless broadband access. Technical report, European Telecommunications Standards Institute.
[8] ETSI (2001). Broadband radio acces network (bran) ; high performance radio local area network (hyperlan] type 2; physical layer. Technical report, European Telecommunications Standards Institute.
[9] Genevieve, B. (2007). Radiocommunications numriques: Tome 1, Principes, modlisation et simulation. Radiocommunications numriques. Dunod, 2 edition.
[10] Hara, S. and Prasad, R. (1997). Overview of multicarrier cdma. Communications Magazine, IEEE, 35(12):126–133.
[11] Le Floch, B., Alard, M., and Berrou, C. (1995). Coded orthogonal frequency division multiplex [tv broadcasting]. Proceedings of the IEEE, 83(6):982–996.
[12] Massiani, A. (2005). Prototyping of high-rate systems based on the combination of multi-carrier modulations, spread spectrum technique and multiple antennas modulations. Theses, INSA de Rennes.
[13] McCormick, A. and Al-Susa, E. (2002). Multicarrier cdma for future generation mobile communication. Electronics Communication Engineering Journal, 14(2):52–60.
[14] Mourad, A.-M. (2006). On the System Level Performance of MC-CDMA Systems in the Downlink. Theses, Ecole Nationale Supérieure des Télécommunications de Bretagne - ENSTB.
[15] Nabiha, S. and Hassani, M. (2009). Supervised equalization of a linear communication channel using generalized orthogonal basis (gob). In Systems, Signals and Devices, 2009. SSD'09. 6th International Multi-Conference on, pages 1–6.
[16] Nathan, Y., Linnartz, J.-P. M., and Fettweis, G. (1994). Multi-carrier cdma in indoor wireless radio networks. IEICE Transactions on Communications, 77(7):900–904.
[17] NOBILET, S. (2003). Etude et optimisation des techniques MC-CDMA pour les futures générations de systèmes de communications hertziennes. Theses, INSA de Rennes.
[18] Peled, A. and Ruiz, A. (1980). Frequency domain data transmission using reduced computational complexity algorithms. In Acoustics, Speech, and Signal Processing, IEEE International Conference on ICASSP '80., volume 5, pages 964–967.
[19] Peng, D., Xiang, Y., and Yi, Z. (2009). A new adaptive blind channel identification algorithm. Chaos, Solitons & Fractals, 41(1):354 – 359.
[20] Perez-Cruz, F. and Bousquet, O. (2004). Kernel methods and their potential use in signal processing. Signal Processing Magazine, IEEE, 21(3):57–65.
[21] Pillonetto, G., Dinuzzo, F., Chen, T., Nicolao, G. D., and Ljung, L. (2014). Kernel methods in system identification, machine learning and function estimation: A survey. Automatica, 50(3):657 – 682.
[22] Pinchon, D., Siohan, P., and Siclet, C. (2004). Design techniques for orthogonal modulated filterbanks based on a compact representation. Signal Processing, IEEE Transactions on, 52(6):1682–1692.
[23] Proakis, J. and Salehi, M. (2007). Digital Communications, pages 642–645. McGraw-Hill higher education. McGraw-Hill Education, fifth edition.
[24] Sadler, B., Giannakis, G., and Lii, K.-S. (1994). Estimation and detection in non-gaussian noise using higher order statistics. Signal Processing, IEEE Transactions on, 42(10):2729–2741.
[25] Safi, S., Frikel, M., Pouliquen, M., Badi, I., Khmou, Y., and Boutalline, M. (2013). Mc-cdma system identification and equalization using the lms algorithm and takagi-sugeno fuzzy system. IFAC Proceedings Volumes, 46(11):599 – 604.
[26] Safi, S., Frikel, M., Zeroual, A., and M'Saad, M. (2011). Higher order cumulants for identification and equalization of multicarrier spreading spectrum systems. Journal of telecommunications and information technology, pages 74–84.
[27] Shawe-Taylor, J. and Cristianini, N. (2004). Kernel Methods for Pattern Analysis. Cambridge University Press.
[28] Skrzypczak, A. (2007). Contribution l'tude des modulations multiporteuses OFDM/OQAM et OFDM surchantillonnes. PhD thesis, Universit de Rennes 1.
[29] Teich, W., Bury, A., Egle, J., Nold, M., and Lindner, J. (1998). Iterative detection algorithms for extended mc-cdma. In Spread Spectrum Techniques and Applications, 1998. Proceedings., 1998 IEEE 5th International Symposium on, volume 1, pages 184–188 vol.1.
[30] Van Vaerenbergh, S. and Azpicueta-Ruiz, L. A. (2014). Kernel-based identification of hammerstein systems for nonlinear acoustic echo-cancellation. In 2014 IEEE International Conference on Acoustics, Speech and Signal Processing (ICASSP).
[31] Van Vaerenbergh, S. and Santamaria, I. (2013). A comparative study of kernel adaptive filtering algorithms. In Digital Signal Processing and Signal Processing Education Meeting (DSP/SPE), 2013 IEEE, pages 181–186.
[32] Vapnik, V. N. (2000). The nature of statistical learning theory. statistics for engineering and information science. Springer-Verlag, New York.
[33] Yong, X., Liu, Y., Dezhong, P., and Shengli, X. (2014). A second-order blind equalization method robust to

illconditioned SIMO FIR channels. Digital Signal Processing, 32(0):57 – 66.